Clim. Past Discuss., doi:10.5194/cp-2017-50, 2017
Manuscript under review for journal Clim. Past
Discussion started: 27 March 2017


Climate of the Past Discussions
Open Access

# Environmental dynamics since the last glacial period in arid Central Asia: evidence from grain size distribution and magnetic properties of loess from the Ili Valley, western China

Yue Li[1,2], Yougui Song[1]*, Kathryn E. Fitzsimmons[3], Hong Chang[1], Rustam Orozbaev[4,5], Xinxin Li [1,2]

1 State Key Laboratory of Loess and Quaternary Geology, Institute of Earth Environment, Chinese Academy of Sciences, Xi'an, 710061, China
2 College of Earth Science, University of Chinese Academy of Sciences, Beijing, 100049, China
3 Research Group for Terrestrial Palaeoclimates, Max Planck Institute for Chemistry, Hahn-Meitner-Weg 1, 55128 Mainz, Germany
4 Research Center for Ecology and Environment of Central Asia, Chinese Academy of Sciences, Urumqi, 830011, China
5 Institute of Geology, National Academy of Sciences, Bishkek, 720040, Kyrgyzstan

* Corresponding author:
Dr. Yougui Song
E-mail: syg@ieecas.cn
State Key Laboratory of Loess and Quaternary Geology
Institute of Earth Environment, Chinese Academy of Sciences
No. 97 Yanxiang Road, Yanta, Xi'an 710061, China
Tel. 86-29 6233 6216
Fax. 86-29 6233 6216

Clim. Past Discuss., doi:10.5194/cp-2017-50, 2017
Manuscript under review for journal Clim. Past
Discussion started: 27 March 2017


Climate of the Past Discussions

**Abstract**

The extensive loess deposits of the Eurasian mid-latitudes provide important terrestrial records of Quaternary climatic change. As yet, however, loess records in Central Asia are poorly understood. Here we investigate the grain size and magnetic characteristics of loess from the Nilka (NLK) section in the Ili Basin of eastern Central Asia. Magnetic parameters indicate very weak pedogenesis compared with loess from other regions in Eurasia. The higher $\chi_{lf}$ values occur in primary loess, rather than in weak paleosols, and the variations in magnetic susceptibility (MS) value correlate closely with the proportions of the sand fraction. We attribute this result to high wind strength at the time of loess deposition. To explore the dust transport patterns further, we identified three grain size end members (EM1, mode size 47.5 μm; EM2, 33.6 μm; EM3, 18.9 μm) which represent distinct aerodynamic environments. EM1 and EM2 represent the grain-size fractions transported from proximal sources in short-term, near-surface suspension during dust outbreaks. EM3 appears to represent the continuous background dust fraction under non-dust storm processes. Of the three end members, EM1 is most likely the most sensitive recorder of wind strength. A lack of correlation between EM1 proportions and GISP $\delta^{18}O$ values at the millennial scale, combined with modern weather data, suggests that Arctic polar front predominates in the Ili Basin and the Kyrgyz Tian Shan piedmont during cold phases, which leads to the dust transport and accumulation of loess deposits, while the shift of mid-latitude westerlies towards the south and north controls the patterns of precipitation/moisture variations in this region. Comparison of EM1 proportions with Northern Hemisphere summer insolation clearly illustrate local insolation-based control on wind dynamics in the region, and humdity can also influence grain size of loess over MIS3 in particular. Although, the polar front dominated wind dynamics for loess deposition in the region, the Central Asian high mountains obstructed its migration further south. Our results may also support the significance of the mid-latitude westerlies in transmitting North Atlantic climate signals to East Asia.

Key words: Last glacial, Ili Basin, Central Asia, loess, magnetic susceptibility, grain size, paleoclimate

## 1 Introduction

Central Eurasia experiences extremely continental climatic conditions in large part due to its position far from oceans. Arid Central Asia is therefore a sensitive recorder of past climate change due to its location in the transition zone between the Asian monsoon (Dettman et al., 2001;Cheng et al., 2012), mid-latitude westerlies (Vandenberghe et al., 2006) and North Asian polar front (Machalett et al., 2008). The relative influence and intensity of these major climate subsystems have varied across the latitudinal and longitudinal range of Central Asia through time. Thus identification of the predominant climate regimes in a certain region is a crucial precondition for tracing paleoclimatic evolution.

One of the most promising potential palaeoenvironmental archives in the Central Asian region is its widespread, thick loess deposits. Loess is one of the most important archives of Quaternary climate change (Maher, 2016;Muhs, 2013). The semi-arid zone of Eurasia, between 45° and 30° N, hosts some of the thickest and most extensive loess deposits in the world. In Central Asia, the loess deposits cover the slopes of the Tian Shan mountains, from Xinjiang province of China and Kazakhstan, to Kyrgyzstan and Uzbekistan, to Tajikistan. While loess in Central Asia has increasingly formed the focus of loess research (Dodonov et al., 2006;Feng et al., 2011;Li et al., 2016c;Li et al., 2016b;Machalett et al., 2006;Smalley et al., 2006;Song et al., 2014;Song et al., 2015;Song et al., 2012;Yang et al., 2006;Youn et al., 2014;Fitzsimmons et al., 2016), as yet the forcing mechanisms and the climatic conditions responsible for loess-paleosol sequences formation are ambiguous, and the paleoclimatic evolution recorded by these loess deposits in this region is not systematically understood.

Evidence for temperature oscillations associated with the Greenland (*Dansgarrd/Oeschger (D-O) events*) (Dansgaard et al., 1993) and cool phases associated with iceberg calving into the North Atlantic (*Heinrich (H) events*) (Bond et al., 1992) have been found in loess deposits based on the high-resolution grain-size variations ether in Chinese Loess Plateau (CLP) loess (Sun et al., 2012;Porter and An, 1995) or in European loess (Antoine et al., 2009;Rousseau et al., 2007;Zeeden et al., 2016). Climatic teleconnections, especially between the North Atlantic and East Asian Monsoon regions, are likely to have been recorded within the Central Asian loess. As yet, however, the region so far largely lacks data by which the role and contribution of the central parts of the Eurasian continent, as an environmental bridge, can be elucidated.

The Ili Basin of Central Asia represents a region of thick loess deposits with high potential for investigating palaeoenvironmental change for the region. The situation of the basin, surrounded to the south and north by the Tian Shan mountain range and widening to the west (Fig. 1), provides a conducive situation for loess accumulation which has resulted in the widespread and thick loess deposits in this basin. In this paper we present new data on the physical properties of a 20.4 m thick loess deposit at Nilka (NLK) in the eastern Ili Basin, focusing on grain size distributions and magnetic properties in order to investigate the enhancement mechanisms of magnetic susceptibility in NLK loess and elucidate environmental dynamics based on grain size data.

## 2 Physical geography

The Ili Basin (80° ~ 85° E and 42° 30′ ~ 44° 30′ N) straddles southeast Kazakhstan and northwest China. It is an intermontane basin opening westward towards the semi-arid Kazakhstan Gobi Desert which forms the transitional region between the steppe and full deserts of Central Asia. The Northern and Southern Tian Shan form the northern and southern boundaries to the basin (Fig. 1a). The Ili River drains northwestward into terminal Lake Balkhash.

This region has a semi-arid, continental climate, with a strong precipitation gradient dependent on altitude. The altitude of the basin floor is 500 ~ 780 m; the northern Tien Shan Range reaches altitudes of > 4000 m a.s.l. and the southern Tien Shan mountains range between 3000 ~7000 m a.s.l. towards the catchment divide. The mean annual precipitation (MAP) ranges between 200 mm and 500 mm on the plains, and mean annual temperature (MAT) ranges from 2.6°C to 10.4°C (Li, 1991;Ye, 1999). The surface vegetation in this region is dominated by *Desert Steppe* and *Steppe* and the zonal soils comprise *Sierozem*, *Castonozem* and *Chernozem*.

The Nilka (NLK) section (83.25°E, 43.76°N, 1253 m a.s.l) is situated on the second terrace of the right bank of the Kashi River, a tributary of the Ili River. The site is located in the eastern Ili Basin of far western China, adjoining the Northern Tian Shan to the north (Fig. 1b).

Fig. 1 The location of study area and the photo of Nilka (NLK) section.

## 3 Materials and methods

### 3.1 Section and sampling

Clim. Past Discuss., doi:10.5194/cp-2017-50, 2017
Manuscript under review for journal Clim. Past
Discussion started: 27 March 2017




The NLK loess section has a thickness of 20.4 m and overlies fluvial sands and gravels (Fig.1). The profile has been exposed recently by local residents for making bricks, and recently formed the focus of a geochronological study comparing luminescence with radiocarbon methods (Song et al., 2015). According to the dating results of Song et al. (2015), the NLK loess started to accumulate since ~ 70 ka B.P.. Stratigraphically and geochronologically, this is equivalent to the L1 loess unit (known as Malan loess) and S0 paleosol unit (known as Holocene Heilu soil) in the Chinese Loess Plateau, 2300 km to the east. Although largely homogeneous in appearance, two weak paleosols (at 5.04 − 7 m and 15.7 − 18 m depths) were identified in the section by field observations and confirmed by our subsequent grain-size and magnetic susceptibility (MS) results. We therefore divided the NLK stratigraphy into S0, L1L1, L1S1, L1L2, L1S2 and L1L3 units (Fig. 1c).

Following cleaning back of the NLK section to remove dry, weathered sediment, samples were collected at intervals of 2 cm. A total of 1026 bulk samples were prepared for measurements of physical characteristics. This study uses the more reliable optically stimulated luminescence (OSL) dating results as basis for the age model and assessment of the evolution of loess physical characteristics.

### 3.2 Grain-size analyses

Prior to grain size measurements, 0.5 g of dry bulk sample was pretreated by removal of organic matter and carbonate using $H_2O_2$ and HCl, respectively (Lu and An, 1997). Samples were then dispersed for 5 min by ultrasonification with 10 ml 10% $(NaPO_3)_6$ solution. Grain size distribution was analysed using a Malvern 2000 laser instrument at the State Key Laboratory of Loess and Quaternary Geology, Institute of Earth Environment, Chinese Academy of Sciences. Particle size distribution was calculated for 100 grain size classes within a measuring range of 0.02−2000 μm. Replicate analyses indicated an analytical error of < 2% for the mean grain size.

End-member unmixing of loess grain-size distributions is based on the hierarchical Bayesian model for end-member modeling analysis (BEMMA) established by Yu et al. (2016). Grain-size parameters were calculated from the analytical data with GRADISTAT (Version 4.0; Blott (2000)).

2 samples (NLK1106 at 11.06 m and NLK1840 at 17.8 m) were also selected for the extraction of quartz grains according to published methods of Sun et al. (2000a). The isolated quartz grain samples (Fig. S1) then placed into the Malvern 2000 laser instrument for mineral-specific grain size measurements so that comparisons of quartz grain and bulk samples could be performed to illustrate the weathering degree of NLK loess visually.

### 3.3 Magnetic susceptibility measurements

Magnetic susceptibility was measured with a Bartington MS2 meter at the State Key laboratory of Loess and Quaternary Geology, Institute of Earth Environment, Chinese Academy of Sciences. Samples were oven-dried at 40°C for 24 hours. Subsamples of 10 g from each sample were then weighed for magnetic measurements. Low- (0.47 kHz) and high- (4.7 kHz) frequency magnetic susceptibility ($\chi_{lf}$ and $\chi_{hf}$, respectively) were measured. The absolute frequency-dependent magnetic susceptibility was calculated as $\chi fd = \chi_{lf} - \chi_{hf.}$ Frequency-dependent magnetic susceptibility was defined and calculated as $\chi_{fd}$ % = $[(\chi_{lf} - \chi_{hf})/ \chi_{lf}] \times 100\%$.

## 4 Results

### 4.1 Magnetic susceptibility variations

Both magnetic susceptibility (MS) data and stratigraphy show a close correspondence throughout the NLK section. We observe higher MS values within primary loess and lower values within paleosols. The exception to this trend is the modern (S0) soil in which high MS values are presented (Fig. 2).

Fig. 2 Lithology and magnetic susceptibility characteristics ($\chi_{lf}$, $\chi_{fd}$ and $\chi_{fd}$%) of the NLK section.

The low-frequency magnetic susceptibility ($\chi_{lf}$) values of the S0 unit are higher than for the L1 unit, with an average of 98.13 × $10^{-8}m^3kg^{-1}$. The $\chi_{lf}$ values of the L1L1 unit vary from 56.5 − 103.9 × $10^{-8}m^3kg^{-1}$, with a decreasing trend down-profile. The $\chi_{lf}$ value abruptly decreases at c. 5 m, with generally lower values in the L1S1 unit, averaging 62.58 × $10^{-8}m^3kg^{-1}$. $\chi_{lf}$ in the L1L2 unit gradually increases down profile, with significant fluctuations in the lower part; $\chi_{lf}$ values vary from 67 − 102.55 × $10^{-8}m^3kg^{-1}$. Lower $\chi_{lf}$ values are observed in L1S1 unit with an average value of 57.99 × $10^{-8}m^3kg^{-1}$. In the L1L3 unit, the $\chi_{lf}$ values vary with greater amplitude around an average value of 68.74 × $10^{-8}m^3kg^{-1}$.

Absolute frequency-dependent magnetic susceptibility ($\chi_{fd}$) values likewise vary with stratigraphy. The S0 unit yields the highest $\chi_{fd}$ value. The L1 unit is characterized by relatively consistent and lower $\chi_{fd}$ values. Frequency-dependent magnetic susceptibility ($\chi_{fd}$%) yields the same trend as $\chi_{fd}$, although $\chi_{fd}$% values clearly increase in the central part of L1S2.

**4.2 Mixing model of loess grain-size distributions**

The mean grain-size distribution, and variation range of volume frequencies for each grain-size class in the dataset, are presented in Fig. 3a. The overall grain-size frequency curve shows a unimodal pattern, if slightly skewed towards the coarser side, with the primary mode ranging from 11.9 µm to 47.5 µm. An additional small grain size peak occurs at c. 0.4 – 2 µm. Three unmixed end members were identified (Fig. S2), yielding fine-skewed grain-size distributions with clearly defined modes of 47.5 µm (EM1), 33.6 µm (EM2) and 18.9 µm (EM3) (Fig. 3b).

Fig. 3 End-member modelling results of the grain-size dataset of the NLK section. (a) Mean size distribution and range of volume frequency for each size class. (b) Modelled end-members according to the three-end-member model (modal size: ~ 47.5 µm, ~ 33.6 µm and ~ 18.9 µm). Size limits of clay, silt and sand fractions determined by laser particle sizer are differ from those derived by the pipette method. The upper limits of grain-size classes used here are at 4.6/5.5 µm for clay, 26 µm for fine silt, and 52 µm for coarse silt, as previously published by Konert and Vandenberghe (1997). Sand is designated for particle sizes > 52 µm. Therefore, EM1 and EM2 correspond to coarse silt and EM3 to fine silt.

Fig. 4 Proportional contributions of the three end-members in the NLK section.

The proportional distribution of the end members down the section is shown in Fig. 4. In the primary loess units (L1L1, L1L2 and L1L3), the deposits are dominated by the coarser silt EM1 and EM2, while higher proportions of fine silt EM3 are preferentially observed within the soil horizons (S0, L1S1 and L1S2). EM1 displays high frequency, large amplitude fluctuations down the profile, varying between 0.09 – 0.72, and clearly dominates the primary loess units and occurs in low proportions in the soil units (Fig. 4). EM2 shows a similar trend to EM1, but with less variability down profile. Proportions of EM2 range between 0.11 − 0.66 with minimal fluctuations within individual units, and proportions decrease significantly in the soil units S0 and L1S2. Proportions of EM3 remain consistently low within the primary loess units, and increase to 0.46 and 0.8 within the soil horizons S0 and L1S2 respectively.

## 5 Discussion

### 5.1 Likely mechanisms for the enhancement of magnetic susceptibility in Ili Basin loess

Magnetic susceptibility (MS) in loess is due to the concentration of iron-bearing magnetic minerals within the sediment (Hambach et al., 2009;Buggle et al., 2014;Liu et al., 1999;Liu et al., 1994;Song et al., 2010). At the broadest level, this varies between primary loess and soil horizons, with soils generally experiencing an enrichment of magnetic minerals, and corresponding higher MS values, than primary loess deposits (Zhou et al., 1990;Maher and Thompson, 1992;Heller and Evans, 1995;Antoine et al., 1999;Heller and Liu, 1984;Ding et al., 2002;Forster and Heller, 1997;Buggle et al., 2009a). The formation *in situ* of < 100 nm magnetite or maghemite grains during pedogenesis is the most widely accepted interpretation for the mechanisms of loess MS enhancement (Nie et al., 2016). Increased precipitation is conducive to chemical weathering and biological processes during pedogenesis. Song et al. (2010) further argued that strong pedogenesis under warm, humid climatic conditions produces new magnetic minerals. The contrast between high and low MS in paleosols and primary loess, respectively, has formed the basis for the stratigraphic differentiation of loess deposits. This principle has provided the foundation for large-scale correlations between loess deposits (Marković et al., 2015;Yang et al., 2006;Ding et al., 2002;Marković et al., 2012;Buggle et al., 2009b;Sun et al., 2006a) and with global climatic oscillations (Bloemendal et al., 1995;An et al., 1991;Kukla et al., 1988;Heller and Liu, 1986;Heller and Liu, 1982), initially in the Chinese Loess Plateau deposits and increasingly worldwide.

The main MS variations in the NLK loess sequence, with the exception of the S0 unit, however, do not occur directly in association with pedogenesis (Fig. 2). A similar case also occurs in the L1 loess layers in TLD, ZKT and AXK sections, also in the Ili valley (Fig. 1) (Jia et al., 2010;Jia et al., 2012;Song et al., 2010). The lack of a straightforward correlation between MS, loess and paleosols indicates that an alternative explanation for this variability must be sought. Proposed mechanisms of variations in loess magnetic susceptibility include, in addition to pedogenesis (Zhou et al., 1990;Maher, 1998), the dilution of relatively coarse silt with a low susceptibility (Kukla and An, 1989), sediment compression and carbonate leaching (Heller and Liu, 1984), and decomposition of plant residues (Meng et al., 1997).

Since alternative mechanisms may have played a role in the magnetization of the Ili Basin loess deposits, we investigated different aspects of environmental magnetic properties in order to investigate to what degree pedogenesis or the alternative mechanisms played the more critical role in this region.

Absolute frequency-dependent susceptibility ($\chi_{fd}$) determines the concentration of magnetic particles within a small grain size range across the superparamagnetic (SP)/stable single domain (SSD) boundary (Liu et al., 2012) (magnetite, < ~100 nm; maghemite, < ~20 μm). Particles with this grain size are considered to form in situ within soils during pedogenesis (Maher and Taylor, 1988;Zhou et al., 1990), and therefore $\chi_{fd}$ can serve as a direct proxy for pedogenesis (Heller et al., 1993;Maher and Thompson, 1995;Liu et al., 2007;Buggle et al., 2014). In the NLK section, $\chi_{fd}$ yields consistently low values throughout the sequence and indicates no clear strong pedogenesis even in the weakly developed paleosol layers (L1S1 and L1S2). Comparison between $\chi_{lf}$ vs. $\chi_{fd}$ down profile shows no correlation between MS and SP particles (Fig, S3c). These results suggest that SP particles played only a minor role in MS enhancement in the NLK loess.

Frequency-dependent magnetic susceptibility ($\chi_{fd}$%) is used as a proxy to determine the contribution of SP particles to MS (Zhou et al., 1990;Liu et al., 1992). At NLK, however, we observe consistently low $\chi_{fd}$% values in both loess and paleosol layers, with a slight increase only in the L1S1 paleosol. This observation reinforces our interpretation that the content of SP particles is very low, and consequently that their contribution to MS can be ignored.

The low proportions of SP particles in the NLK loess imply that the pseudo-single-domain (PSD) and multi-domain (MD) magnetic grains, rather than SP grains, make the more important contribution to magnetic enhancement of NLK loess. Since PSD and MD magnetic minerals are difficult to produce during pedogenesis (Song et al., 2010), such minerals are more likely to be detrital in nature, deriving from the original protolith.

Fig. 5 Comparison of different grain size fractions of NLK loess with $\chi_{lf}$ (limits of grain-size classes after Konert and Vandenberghe (1997) ).

In some cases, the moist conditions typically conducive to pedogenesis, including high precipitation and rising groundwater levels, may result in the weathering, destruction and dissolution of the magnetic minerals maghemite and magnetite (Nawrocki et al., 1996;Cornell and Schwertmann, 2003;Maher, 1998;Grimley and Arruda, 2007;Hu et al., 2009b;Hu et al., 2009a;Ghafarpour et al., 2016). In such cases, a negative relationship between magnetic susceptibility and pedogenesis can develop, in contrast to the classical situation whereby $\chi_{fd}$ is enhanced. At NLK, however, we observe no textures caused by groundwater fluctuations, and yet very weak pedogenesis was reflected by $\chi_{fd}$. We therefore exclude groundwater fluctuations and high levels of precipitation as a factor in our MS characteristics at NLK.

Increased concentrations of coarser-grained detrital magnetic minerals, resulting from periods of increased wind strength, may enhance overall MS values. In the wind velocity/vigor model (also known as the Alaskan or Siberian model), wind strength affects magnetic susceptibility values of loess through the physical sorting of magnetic grains (Beget and Hawkins, 1989). The influence of this process on MS values in loess can be assessed by investigating the correlation between MS and coarser (silt or sand) and finer clay percentages (Fig. S3). At NLK, low MS values in the S0 soil between 0 – 0.5 m correlate positively with clay percentage variations (Fig. S3a), while higher MS values at depths greater than > 0.5 m correlate closely with increased sand concentrations (Fig. S3b). We therefore propose that MS enhancement at NLK is primarily driven by increased concentrations of sand-sized detrital magnetic minerals, which increase during periods of stronger winds. The dilution effect of coarse particles with low susceptibility was excluded.

In the case of NLK, the reduced color contrast (Fig. 1) between loess and paleosol layers implies moderate climate fluctuations between loess deposition and pedogenesis due to generally more arid conditions than typically experienced in loess regions. This prevents the efficient production of SP grains (Fig. 2). Wind strength can therefore be regarded as a main factor for MS variations since last glacial. And in turn, MS may be able to indicate stronger wind during dust storms.

**5.2 Genetic interpretations of end members in loess grain size**

In order to understand the atmospheric dynamic pattern during loess deposition further, we conducted unmixing of grain-size distributions.

Recent years have seen increasing statistical analysis of loess grain-size to identify subpopulations within bulk samples (Prins, 2007;Prins et al., 2007;Qin et al., 2005;Sun et al.,

Clim. Past Discuss., doi:10.5194/cp-2017-50, 2017
Manuscript under review for journal Clim. Past
Discussion started: 27 March 2017




2002;Vriend et al., 2011;Vandenberghe, 2013;Sun, 2004). From these statistical datasets, the different end members can be interpreted to infer distinct atmospheric transport mechanisms, modes and travel distances (Ujvari et al., 2016). In some cases, the end-member approach has been used to identify variation in geological context, or source area (Prins et al., 2007). We investigated the utility of this approach to the Ili Basin loess at NLK by unmixing grain-size distributions with BEMMA (Yu et al., 2016). As shown in Fig. S2, we generated a mixing model consisting of three end members.

Fine sand ('*sediment type 1.a*' in Vandenberghe (2013)) is a typical component of loess deposits near to or overlying river terraces. Although the NLK section lies on the second terrace of the Kashi River and therefore closer to a potential source of coarser grained material, the fine-sand end member is completely absent. Modal grain sizes in this range (c. 75 um) are common in loess along the Huang Shui and Yellow Rivers in China (Vriend and Prins, 2005;Vandenberghe et al., 2006;Prins et al., 2009), the Danube and Tisza rivers in Serbia (Bokhorst et al., 2011), and the Mississippi valley in the USA (Jacobs et al., 2011). This fraction is generally interpreted to originate from proximal sources, and the grain size of the available source material plays a more important role in determining the grain-size characteristics of this fraction than wind energy (Vandenberghe, 2013). The lack of fine sand at NLK, despite its proximity to the Kashi River, may be attributed to 1) its location in the upper reaches of the river (Fig. 1b), in a region which lacks available stocks of fine sand, 2) the V-shaped nature of the channel which is not conducive to aeolian transport of bank deposits, and 3) the relatively high altitude of NLK within the basin which inhibits transport and deposition of coarser sediment grains (Vandenberghe, 2013).

The three members (Fig. 3b) identified at NLK correspond to coarse silt (EM1 and EM2) and fine silt (EM3). Each likely represent different kinds of depositional processes which operated throughout the accumulation of the deposit at NLK. Here we focus on the implications of these three end members for understanding past environmental conditions responsible for loess-paleosol sequences formation.

EM1 has a modal grain size of 47.5 µm (Fig. 3b), which approximately corresponds to the '*subgroup 1.b.1*' of Vandenberghe (2013). The mode is similar to end members identified in loess from the Chinese Loess Plateau (CLP) and the north-eastern Tibetan Plateau (NE-TP) (EM-2: 44 µm) (Vriend et al., 2011). The size of this component is unlikely to be due to longer distance transport. Therefore it is inferred that EM1 is derived from shorter distance transport of suspended load (Vriend et al., 2011;Vandenberghe et al., 2006). Coarser particles with grain-size >20 um rarely reach suspension above the near surface level (0 − 200 m above the ground). When entrained by wind, they do not remain in suspension for long enough to travel long distances (Tsoar and Pye, 1987;Pye, 1987). Since the average grain-size of EM1 is 26.74 µm (calculated after Folk and Ward (1957)), we infer that this fraction was transported mainly in short-term suspension episodes at lower elevations by surface winds, and deposited short distances downwind of the source. These short-term suspension episodes may correspond to spring-summer dust storms, as demonstrated by present-day dust measurements on the CLP which detected a similar modal grain-size during these events (Sun et al 2003).

EM2 represents a mode at 33.6 µm (Fig. 3b). It lies towards the finer end of the range of '*subgroup 1.b.2*' (Vandenberghe, 2013). Comparable loess of the same grain size has been identified in loess from the northern Qilian Shan/Hexi Corridor (EM-2: 33 µm), which was also interpreted as depositing from short-term suspension (Nottebaum et al., 2015). Loess of this grain size has been attributed to dust fallout (Pye, 1995;Muhs and Bettis, 2003) and from low-altitude suspension clouds (Sun et al., 2003), as measured from modern depositional events. This fraction requires less wind energy than EM1, is transported further, is more widely distributed, and therefore comprises a higher proportion of the distally deposited population in loess generally (Vandenberghe, 2013). We propose that EM2 was transported mainly in short-term, near-surface suspension during dust storms, and that wind strength controlled the relative proportions of EM1 and EM2 through time (see the mirror image relationships over millennial scales in Fig. 4), which may implied that both EM1 and EM2 have a same origin.

The grain-size distribution of EM3 has a modal peak at 18.9 µm (Fig. 3b). This population belongs to '*subgroup 1.c.1*' in Vandenberghe (2013). This population is also widespread in loess from the CLP and northeastern Tibetan Plateau (Prins et al., 2007;Prins, 2007), and the Danube Basin loess of Europe (Bokhorst et al., 2011;Varga, 2011), particularly in loess of interglacial age (Vriend, 2007). There is as yet no consensus as to the transport processes responsible for this grain size population. On the one hand, researchers have suggested that grains of this size can be lifted by strong vertical air movement and subsequently incorporated into the high-level westerly air streams (Pye, 1995;Pye and Zhou, 1989). This process would link EM3 with long-term suspension transport driven by high-level Westerlies (Prins et al., 2007;Vriend et al., 2011;Nottebaum et al., 2014;Vandenberghe, 2013). Conversely, Zhang et al. (1999) argued that EM3 derives from "non-dust storm processes" associated with north-westerly surface winds. We argue for the latter on the basis that the EM3 modal grain size from the CLP and northeast Tibetan Plateau is coarser (Vriend et al., 2011) than EM3 at NLK in the Ili Valley, which is located further west. If EM3 was transported by high-level westerlies, then one would expect either no significant change (Rea et al., 1985;Rea and Hovan, 1995), or a decrease in grain size from west to east concomitant with wind direction. Furthermore, with mathematical fitting, Sun et al. (2004) related a fine component (2 – 8 µm) to high-altitude westerlies. This fine component is comparable to '*subgroup 1.c.2*' of Vandenberghe (2013), which is not consistent with the modal size of EM3. Observations of modern aeolian processes at the southern margins of the Tarim Basin indicate that fine grain sizes similar to EM3 (8 − 15um) are deposited by settling during low velocity wind conditions (Lin et al., 2016). We therefore infer the EM3 modal peak to derive from low altitude non-dust storm processes.

Other possibilities for the deposition of the fine particles include the incorporation into silt- or sand-sized aggregates which can be transported by a range of wind velocities including dust storms (Qiang et al., 2010;Pye, 1995;Derbyshire et al., 1998;Mason et al., 2003). For example, Ujvari et al. (2016) indicated that the ~ 1 – 20 µm fractions are affected by aggregation by comparison between minimally and fully dispersed grain size distributions of loess samples from southern Hungary. Under higher wind velocity conditions, the aggregate model should co-vary with the coarser EM1 particles which were transported by surface winds during dust storms. However, since this model is unlikely to hold for EM3 particles (Fig. 4), the aggregate model is not thought to be responsible for the presence of grain sizes corresponding to EM3.

In addition, post-depositional processes may also influence grain size distribution. In large part this occurs by chemical weathering which produces very fine silt and clay minerals (Xiao et al., 1995;Wang et al., 2006;Hao et al., 2008). In particular, quartz grains are more weathering resistant and remain largely unaltered during the post-depositional processes. Consequently, quartz mineral grain size may be used as a more reliable proxy indicator of winter monsoon strength than other components (Sun et al., 2006b;Sun et al., 2000b;Xiao et al., 1995).

Figure. 6a shows the grain size distribution curves of quartz grains isolated from primary loess (yellow) and paleosol (red) samples. The quartz modal grain size is finer in the paleosol than in the primary loess unit. From this we can deduce that wind strength was weaker during pedogenesis, and stronger during periods of primary loess deposition. The grain size distributions of bulk samples display similar characteristics with those of quartz samples mentioned above (Fig. 6b), whereby soil unit modal peaks (red and orange) are finer than those for primary loess (blue and green). Therefore, we argue that wind strength, rather than the post-depositional pedogenesis, has the greatest influence on grain size distribution at NLK, and that EM3 was also not produced by chemical weathering.

Fig. 6 Comparison of grain size distribution between purified quartz subsamples of paleosol and primary loess (a), and between bulk samples of paleosols and primary loess (b). Comparison of the grain size distribution between EM3 and samples from weak paleosol units (c).

The relative proportions of the end members down profile can yield further information about temporal variability in wind dynamics. The fairly consistent proportions of EM3 within the loess units indicate it to represent continuous background dust through time (Vandenberghe, 2013). Proportions of EM1 and EM2 decrease noticeably within paleosol units relative to EM3 (Fig. 4). This indicates that variations in proportions of EM3 are mainly driven by variability of EM1 and EM2 (Vriend et al., 2011), but also that a background sedimentation of EM3 was dominant during weak pedogenesis (Fig. 6c). This characteristic is comparable with observations from the CLP (Zhang et al., 1999).

In addition, small peaks at c. 0.8 μm are also observed in the grain-size distribution curves of all three end members. The generation of finest grain peaks may be due to post-depositional pedogenesis (Sun, 2006), especially for the particles with grain-size smaller than 2 μm (Bronger and Heinkele, 1990;Sun, 2006). Nevertheless, post-depositional weathering is unlikely to have had a significant influence on the populations of EM1, EM2 or EM3, since the dominant modal peaks are much coarser. Other potential sources include transportation as aggregates or by the finest grains adhering to coarser particles during transport. Regardless of cause, these particles are unlikely to yield meaningful information about variability in westerly wind system strength since they do not yield a clear independent end member peak.

### 5.3 Aeolian dust dynamics in eastern Central Asia: links to atmospheric systems

Variations in grain size through time at NLK were largely driven by changes in wind strength, without substantial influence of post-depositional pedogenesis. At NLK, grain size therefore is an indicator for response to the atmospheric system.

The three end members are interpreted to represent different depositional processes which operated throughout the accumulation of the deposit. The finer EM3 is interpreted to represent constant background dust, which continued to accumulate throughout periods of relative stability and pedogenesis. The coarser populations, EM1 and EM2, were transported by low-level winds during major dust storms. EM1 is most likely the most sensitive recorder of wind intensity, since EM2 is less sensitive to wind speeds than EM1 by observation of variations in EM2 proportions throughout L1S1 and L1L2 (Fig. 4).

Fig. 7 Comparison between EM1 grain size variability with the timing of glacial advances in the Tian Shan (Koppes et al. 2008; Owen and Dortch, 2014); stable oxygen isotope variations from the

Clim. Past Discuss., doi:10.5194/cp-2017-50, 2017
Manuscript under review for journal Clim. Past
Discussion started: 27 March 2017

Climate of the Past Discussions

Greenland ice cores (Rasmussen et al., 2014) and insolation values at 45°N (Berger and Loutre, 1991).

From the OSL data (Song et al., 2015), we used linear regression (Stevens et al., 2016) to construct age–depth relationships over intervals of visually similar sedimentation rate (Fig. S4 and Table S1). Based on the independent chronology sequences, we assess the degree of correlation between wind strength variability in the Ili Valley (NLK), as represented by the proportions of EM1, the stable oxygen isotope record from the Greenland ice cores representing North Atlantic paleoclimate (Rasmussen et al., 2014), insolation values at 45°N (Berger and Loutre, 1991) and glacial advances in the Tian Shan (Owen and Dortch, 2014;Koppes et al., 2008) (Fig. 7).

In Fig. 7, EM1 occurs in larger proportions during mid-MIS3, with a higher rate of sedimentary accumulation. Glaciers expanded during early- and late-MIS3 (Owen and Dortch, 2014). Generally dust is assumed to be generated, and deposited, during dry-windy glacial conditions, while interglacial conditions were comparatively wetter and more conductive to pedogenesis (Stevens et al., 2013;Sun et al., 2010;Ding et al., 2002;Dodonov and Baiguzina, 1995). By contrast, a seesaw relationship between rapid loess deposition and glacial expansion was observed during MIS3 from our results (Fig. 7), a model that has also been noticed by Youn et al. (2014). The mass accumulation rate (MAR) of loess is good proxy for aridity (Pye, 1995), while moisture availability is the dominant factor controlling glacier growth in Central Asia, especially for glaciers in the Tian Shan (Zech, 2012;Koppes et al., 2008). We infer, therefore, that moisture had an important impact on accumulation of dust in the study area over MIS3 in particular.

Central Asia is variably influenced by the Asian monsoon from the south (Dettman et al., 2001;Cheng et al., 2012), the mid-latitude westerlies (Vandenberghe et al., 2006), the Siberian high-pressure systems from the northeast (Youn et al., 2014), and the polar front from the north (Machalett et al., 2008). However, by virtue of its geographical position, most of these climate influences can be excluded for the Ili Valley since it is sheltered to the northeast, east and south.. The Asian high mountains largely inhibit the intrusion of Asian (Indian and East Asian) monsoons to the region, and the influence of the Siberian High (An, 2000) has been shown to decrease westward from the CLP (Vandenberghe et al., 2006).

Modern satellite data indicates that dust storm development in Ili river valley is closely linked with southward-moving high-latitude air masses (Ye et al., 2003). Karger et al. (2016) provided a detailed picture of the westerlies for the Ili Basin, in which a rain belt gradually migrated towards the south and north in autumn and summer, respectively. According to this scenario, enhanced evaporation coupled with strengthened westerly winds would bring more humid and warm air masses to Arid Central Asia (ACA) during the Holocene (Zhang et al., 2016). Therefore, based on our grain-size observations, we argue that the Arctic polar front, intruding southward in the winter and retracting northward in summer (Machalett et al., 2008), most likely increased the frequency and strength of cyclonic storms, leading to dust transport and the accumulation of loess deposits during cold phases when it predominated in the Ili Basin and along the Kyrgyz Tian Shan piedmont. While the mid-latitude westerlies increasingly influenced the climate in this region as the climate became warmer when the polar front shifted northward, and controlled the patterns of moisture variations (Huang et al., 2015;Li et al., 2011).

Comparison of EM1 proportions with variability in June insolation at 45ºN shows a distinct correlative relationship on the orbital timescale (Fig. 7), which indicates local insolation-based control on wind dynamics. When the insolation values increases, the rising of temperature, as a result, enhances the frequency or strength of cyclonic storms, resulting in higher sedimentary rates or higher coarse-grain proportions (Fig. 7). However, EM1 proportions exhibit more substantial fluctuations than may be attributed to insolation values during the mid- and late-MIS3. We ascribe that to the humidity variations in the study area. In the early-MIS 3, increased moistures due to migration of westerlies towards the north were conducive to vegetation growth in source areas, which reduced sediment entrainment and resulted in less contribution of coarse grains to loess site, though glacial grinding of rocks in the high mountains could produce amount of fine-grained materials (Smalley, 1995;Li et al., 2016a;Fitzsimmons et al., 2016). Whereas arid environment in the mid-MIS 3, observed by a lack of glacial advance in Tian Shan (Fig. 7) and also reflected by the increased MAR (Fig. 7) (Pye, 1995), likely made these sediments with coarser grain size produced in the early-MIS 3 available as the source materials for NLK loess, as the case in the north-eastern Tibetan Plateau (Vriend et al., 2011).

Over millennial scales, our grain-size proxy data do not correlate strongly with abrupt events, such as H1, H2, H3 and H5, identified from the North Atlantic records (Fig. 7). Some of the peaks in EM1 curve correspond to valleys in GISP $\delta^{18}O$ curve (black arrows in Fig. 7), yet many do not.

Grain size studies of the Darai Kalon loess section in Tajikistan, 1200 km to the southwest of NLK, inferred a strong influence from the westerlies resulting in transport of the North Atlantic signal to the East Asia (Vandenberghe et al., 2006;Porter and An, 1995;Sun et al., 2012). Darai Kalon is, however, located in a region where the mid-latitude westerlies clearly have a much stronger influence. Our results from the Ili Basin contradict those of Vandenberghe et al. (2006), which suggest that the mid-latitude westerlies probably did not predominate north of the Kyrgyz Tian Shan. In this case, the high mountains in Central Asia most likely obstructed the migration of the Asiatic polar front further south towards Tajikistan where those data were derived, thereby resulting in a stronger westerlies signal at Darai Kalon than at NLK.

Our results also contradict those of Yang and Ding (2014), who proposed that millennial-scale North Atlantic climate signals might have been transmitted to the Siberian High via the Barents and Kara Sea ice sheets, and then propagated eastwards to the Chinese Loess Plateau via the winter monsoon system. In our case, the influence from northern climate subsystems such as the Siberian High or polar front appear not to have transmitted millennial-scale North Atlantic climatic events, maybe supporting the significance of the westerlies in transmitting North Atlantic climate signals to East Asia.

**Conclusion**

In this study, a paleoenvironmental record for the last glacial from the Nilka (NLK) loess section in Ili Basin was provided. The magnetic properties of the loess indicate that no strong pedogenesis occurred in this section, even in the paleosol units. Variations in magnetic susceptibility (MS) value closely correlate with the proportions of sand fraction, and wind strength is mainly responsible for those variations since the last glacial.

With the unmixing of grain size distributions, three end members were distinguished: EM1 (mode size at 47.5 μm), EM2 (33.6 μm) and EM3 (18.9 μm). They are indicative of different kinds of depositional processes which operated throughout the accumulation of the loess deposit at NLK. EM1 and EM2 represented the grain-size fractions transported from proximal sources in short-term, near-surface suspension during dust outbreaks. They may have the same origin. While wind strength controls relative proportions, EM1 is most likely the most sensitive recorder of wind strength. EM3 represents continuous background dust under the non-dust storm processes.

The Arctic polar front predominates in the Ili Basin and the Kyrgyz Tian Shan piedmont during cold phases, which leads to the dust transport and increased accumulation of loess deposits, while the shift of mid-latitude westerlies towards the south and north controlled the patterns of precipitation/moisture variations in this region. On the orbital scale, the local insolation-based control has an important impact on wind dynamics directly related to accumulation of loess, and moisture can may also influence grain size of loess in the study area over MIS3 in particular. Although, the polar front dominated wind dynamics for loess deposition in the Ili Basin and the Kyrgyz Tian Shan, the Central Asian high mountains obstructed its migration further south. Our results may also support the significance of the mid-latitude westerlies in transmitting North Atlantic climate signals to East Asia.

**Acknowledgements**

The project is supported by the National Basic Research Program of China (Nos: 2016YFA0601902, 2013CB955904), Natural Science Foundation of China (Nos: 41572162, 41290253), and International partnership Program of Chinese Academy of Science [No: 132B61KYS20160002]. The authors thank Yun Li and Junchao Dong from Institute of Earth Environment, Chinese Academy of Sciences, for their assistances in sampling and experiment, and Jia Li from Xiamen University for her assistance in mathematical treatment.

**References**

An, Z. H., Kukla, G. J., Porter, S. C., and Xiao, J. L.: Magnetic-Susceptibility Evidence of Monsoon Variation on the Loess Plateau of Central China during the Last 130,000 Years, Quaternary Research, 36, 29-36, Doi 10.1016/0033-5894(91)90015-W, 1991.

An, Z. S.: The history and variability of the East Asian paleomonsoon climate, Quaternary Sci Rev, 19, 171-187, Doi 10.1016/S0277-3791(99)00060-8, 2000.

Antoine, P., Rousseau, D. D., Lautridou, J. P., and Hatte´, C.: Last interglacial–glacial climatic cycle in loess-palaeosol successions of north-western France, Boreas, 28, 551–563, 1999.

Antoine, P., Rousseau, D.-D., Moine, O., Kunesch, S., Hatté, C., Lang, A., Tissoux, H., and Zöller, L.: Rapid and cyclic aeolian deposition during the Last Glacial in European loess: a high-resolution record from Nussloch, Germany, Quaternary Sci Rev, 28, 2955-2973, 2009.

Beget, J. E., and Hawkins, D. B.: Influence of Orbital Parameters on Pleistocene Loess Deposition in Central Alaska, Nature, 337, 151-153, DOI 10.1038/337151a0, 1989.

Berger, A., and Loutre, M. F.: Insolation Values for the Climate of the Last 10000000 Years, Quaternary Sci Rev, 10, 297-317, Doi 10.1016/0277-3791(91)90033-Q, 1991.

Bloemendal, J., Liu, X. M., and Rolph, T. C.: Correlation of the Magnetic-Susceptibility Stratigraphy of Chinese Loess and the Marine Oxygen-Isotope Record - Chronological and Paleoclimatic Implications, Earth and Planetary Science Letters, 131, 371-380, Doi 10.1016/0012-821x(95)00016-6, 1995.

Bokhorst, M. P., Vandenberghe, J., Sumegi, P., Lanczont, M., Gerasimenko, N. P., Matviishina, Z. N., Markovic, S. B., and Frechen, M.: Atmospheric circulation patterns in central and eastern Europe during the Weichselian Pleniglacial inferred from loess grain-size records, Quatern Int, 234, 62-74, 10.1016/j.quaint2010.07.018, 2011.

Bond, G., Heinrich, H., Broecker, W., Labeyrie, L., Mcmanus, J., Andrews, J., Huon, S., Jantschik, R., Clasen, S., Simet, C., Tedesco, K., Klas, M., Bonani, G., and Ivy, S.: Evidence for massive discharges of icebergs into the North Atlantic Ocean during the last glacial period, Nature, 360, 245–249, 1992.

Bronger, A., and Heinkele, T.: Mineralogical and clay mineralogical aspects of loess research, Quatern Int, 7, 37-51, 1990.

Buggle, B., Hambach, U., Glaser, B., Gerasimenko, N., Markovic, S., Glaser, I., and Zöller, L.: Stratigraphy, and spatial and temporal paleocliamtic trends in Southeastern/Eastern European loess-paleosol sequences, Quatern Int, 196, 86–106, 2009a.

Buggle, B., Hambach, U., Glaser, B., Gerasimenko, N., Marković, S., Glaser, I., and Zöller, L.: Stratigraphy, and spatial and temporal paleoclimatic trends in Southeastern/Eastern European loess–paleosol sequences, Quatern Int, 196, 86-106, 2009b.

Buggle, B., Hambach, U., Muller, K., Zoller, L., Markovic, S. B., and Glaser, B.: Iron mineralogical proxies and Quaternary climate change in SE-European loess-paleosol sequences, Catena, 117, 4-22, 10.1016/j.catena.2013.06.012, 2014.

Cheng, H., Zhang, P. Z., Spotl, C., Edwards, R. L., Cai, Y. J., Zhang, D. Z., Sang, W. C., Tan, M., and An, Z. S.: The climatic cyclicity in semiarid-arid central Asia over the past 500,000 years, Geophys Res Lett, 39, Artn L01705 10.1029/2011gl050202, 2012.

Cornell, R. M., and Schwertmann, U.: The Iron Oxides, second ed, in, John Wiley, New York, 664, 2003.

Dansgaard, W., Johnsen, S. J., Clausen, H. B., Hvidberg, C. S., and Steffensen, J. P.: Evidence for general instability of past climate from a 250-kyr ice-core record, Nature, 364, 218– 220, 1993.

Derbyshire, E., Meng, X. M., and Kemp, R. A.: Provenance, transport and characteristics of modern aeolian dust in western Gansu Province, China, and interpretation of the Quaternary loess record, J Arid Environ, 39, 497-516, DOI 10.1006/jare.1997.0369, 1998.

Dettman, D. L., Kohn, M. J., Quade, J., Ryerson, F. J., Ojha, T. P., and Hamidullah, S.: Seasonal stable isotope evidence for a strong Asian monsoon throughout the past 10.7 m.y., Geology, 29, 31-34, Doi 10.1130/0091-7613(2001)029<0031:Ssiefa>2.0.Co;2, 2001.

Ding, Z. L., Ranov, V., Yang, S. L., Finaev, A., Han, J. M., and Wang, G. A.: The loess record in southern Tajikistan and correlation with Chinese loess, Earth and Planetary Science Letters, 200, 387-400, doi: DOI: 10.1016/S0012-821X(02)00637-4, 2002.

Dodonov, A. E., and Baiguzina, L. L.: Loess stratigraphy of Central Asia: Palaeoclimatic and palaeoenvironmental aspects, Quaternary Sci Rev, 14, 707-720, http://dx.doi.org/10.1016/0277-3791(95)00054-2, 1995.

Dodonov, A. E., Sadchikova, T. A., Sedov, S. N., Simakova, A. N., and Zhou, L. P.: Multidisciplinary approach for paleoenvironmental reconstruction in loess-paleosol studies of the Darai Kalon section, Southern Tajikistan, Quatern Int, 152, 48-58, 10.1016/j.quaint.2005.12.001, 2006.

Feng, Z. D., Ran, M., Yang, Q. L., Zhai, X. W., Wang, W., Zhang, X. S., and Huang, C. Q.: Stratigraphies and chronologies of late Quaternary loess-paleosol sequences in the core area of the central Asian arid zone, Quatern Int, 240, 156-166, doi: 10.1016/j.quaint.2010.10.019, 2011.

Fitzsimmons, K. E., Sprafke, T., Zielhofer, C., Günter, C., Deom, J. M., Sala, R., and Iovita, R.: Loess accumulation in the Tian Shan piedmont: Implications for palaeoenvironmental change in arid Central Asia, Quatern Int, 1-14, 2016.

Folk, R. L., and Ward, W. C.: Brazos River bar: a study in the significance of grain size parameters, Journal of Sedimentary Research, 27, 3-26, 1957.

Forster, T., and Heller, F.: Magnetic enhancement paths in loess sediments from Tajikistan, China and Hungary, Geophys Res Lett, 24, 17–20, 1997.

Ghafarpour, A., Khormali, F., Balsam, W., Karimi, A., and Ayoubi, S.: Climatic interpretation of loess-paleosol sequences at Mobarakabad and Aghband, Northern Iran, Quaternary Research, 86, 95-109, 10.1016/j.ygres.2016.05.004, 2016.

Grimley, D. A., and Arruda, N. K.: Observations of magnetite dissolution in poorly drained soils, Soil Sci, 172, 968-982, 10.1097/ss.0b013e3181586b77, 2007.

Hambach, U., Jovanovic, M., Markovic, S. B., Nowaczyk, N., and Rolf, C.: The Matuyama-Brunhes geomagnetic reversal in the Stari Slankamen loess section (Vojvodina, Serbia): Its detailed record and its stratigraphic position, EGU General Assembly Conference Abstracts, 11, 11498, 2009.

Hao, Q. Z., Oldfield, F., Bloemendal, J., and Guo, Z. T.: Particle size separation and evidence for pedogenesis in samples from the Chinese Loess Plateau spanning the past 22 m.y., Geology, 36, 727-730, 10.1130/G24940a.1, 2008.

Heller, F., and Liu, T. S.: Magnetostratigraphical Dating of Loess Deposits in China, Nature, 300, 431-433, DOI 10.1038/300431a0, 1982.

Heller, F., and Liu, T. S.: Magnetism of Chinese Loess Deposits, Geophys J Roy Astr S, 77, 125-&, DOI 10.1111/j.1365-246X.1984.tb01928.x, 1984.

Heller, F., and Liu, T.: Palaeoclimatic and sedimentary history from magnetic susceptibility of loess in China, Geophys Res Lett, 13, 1169-1172, 1986.

Heller, F., Shen, C. D., Beer, J., Liu, X. M., Liu, T. S., Bronger, A., Suter, M., and Bonani, G.: Quantitative Estimates of Pedogenic Ferromagnetic Mineral Formation in Chinese Loess and Paleoclimatic Implications, Earth and Planetary Science Letters, 114, 385-390, Doi 10.1016/0012-821x(93)90038-B, 1993.

Heller, F., and Evans, M. E.: Loess magnetism, Reviews of Geophysics, 33, 211–240, 1995.

Hu, X. F., Wei, J., Xu, L. F., Zhang, G. L., and Zhang, W. G.: Magnetic susceptibility of the Quaternary Red Clay in subtropical China and its paleoenvironmental implications, Palaeogeogr Palaeocl, 279, 216-232, 10.1016/j.palaeo.2009.05.016, 2009a.

Hu, X. F., Xu, L. F., Pan, Y., and Shen, M. N.: Influence of the aging of Fe oxides on the decline of magnetic susceptibility of the Tertiary red clay in the Chinese Loess Plateau, Quatern Int, 209, 22-30, 10.1016/j.quaint.2009.02.019, 2009b.

Huang, W., Chen, J. H., Zhang, X. J., Feng, S., and Chen, F. H.: Definition of the core zone of the "westerlies-dominated climatic regime", and its controlling factors during the instrumental period, Sci China Earth Sci, 58, 676-684, 10.1007/s11430-015-5057-y, 2015.

Jacobs, P. M., Mason, J. A., and Hanson, P. R.: Mississippi Valley regional source of loess on the southern Green Bay Lobe land surface, Wisconsin, Quaternary Research, 75, 574-583, 10.1016/j.yqres.2011.02.003, 2011.

Jia, J., Xia, D. S., Wei, H. T., Wang, B., and Liu, X. B.: A magnetic investigation of a loess/paleosol sequences record in Ili area, Front Earth Sci-Prc, 4, 259-268, 10.1007/s11707-010-0115-4, 2010.

Jia, J., Xia, D. S., Wang, B., Wei, H. T., and Liu, X. B.: Magnetic investigation of Late Quaternary loess deposition, Ili area, China, Quatern Int, 250, 84-92, 10.1016/j.quaint.2011.06.018, 2012.

Karger, D. N., Conrad, O., Böhner, J., Kawohl, T., Kreft, H., Soria-Auza, R. W., Zimmermann, N., Linder, H. P., and Kessler, M.: Climatologies at high resolution for the Earth land surface areas, arXiv:1607.00217, 2016.

Konert, M., and Vandenberghe, J.: Comparison of laser grain size analysis with pipette and sieve analysis: A solution for the underestimation of the clay fraction, Sedimentology, 44, 523-535, DOI 10.1046/j.1365-3091.1997.d01-38.x, 1997.

Koppes, M., Gillespie, A. R., Burke, R. M., Thompson, S. C., and Stone, J.: Late Quaternary glaciation in the Kyrgyz Tien Shan, Quaternary Sci Rev, 27, 846-866, 10.1016/j.quascirev.2008.01.009, 2008.

Kukla, G., Heller, F., Ming, L. X., Chun, X. T., Sheng, L. T., and Sheng, A. Z.: Pleistocene Climates in China Dated by Magnetic-Susceptibility, Geology, 16, 811-814, Doi 10.1130/0091-7613(1988)016<0811:Pcicdb>2.3.Co;2, 1988.

Kukla, G., and An, Z. S.: Loess Stratigraphy in Central China, Palaeogeogr Palaeocl, 72, 203-225, Doi 10.1016/0031-0182(89)90143-0, 1989.

Li, G. Q., Rao, Z. G., Duan, Y. W., Xia, D. S., Wang, L. B., Madsen, D. B., Jia, J., Wei, H. T., Qiang, M. R., Chen, J. H., and Chen, F. H.: Paleoenvironmental changes recorded in a luminescence dated loess/paleosol sequence from the Tianshan Mountains, arid central Asia, since the Penultimate Glaciation, Earth and Planetary Science Letters, 448, 1-12, 10.1016/j.epsl.2016.05.008, 2016a.

Li, J.: Climate in Xinjiang, in, China Meteorological Press, Beijing, 1-205 (in Chinese), 1991.

Li, X., Zhao, K., Dodson, J., and Zhou, X.: Moisture dynamics in central Asia for the last 15 kyr: new evidence from Yili Valley, Xinjiang, NW China, Quaternary Sci Rev, 30, 3457-3466, 2011.

Li, Y., Song, Y., Lai, Z., Han, L., and An, Z.: Rapid and cyclic dust accumulation during MIS 2 in Central Asia inferred from loess OSL dating and grain-size analysis, Scientific Reports, 6, DOI: 10.1038/srep32365, 2016b.

Li, Y., Song, Y. G., Chen, X. L., Li, J. C., Mamadjanov, Y., and Aminov, J.: Geochemical composition of Tajikistan loess and its provenance implications, Palaeogeogr Palaeocl, 446, 186-194, 10.1016/j.palaeo.2016.01.025, 2016c.

Lin, Y. C., Mu, G. J., Xu, L. S., and Zhao, X.: The origin of bimodal grain-size distribution for aeolian deposits, Aeolian Research, 20, 80-88, 10.1016/j.aeolia.2015.12.001, 2016.

Liu, Q. S., Deng, C. L., Torrent, J., and Zhu, R. X.: Review of recent developments in mineral magnetism of the Chinese loess, Quaternary Sci Rev, 26, 368-385, 10.1016/j.quascirev.2006.08.004, 2007.

Liu, Q. S., Roberts, A. P., Larrasoana, J. C., Banerjee, S. K., Guyodo, Y., Tauxe, L., and Oldfield, F.: Environmental Magnetism: Principles and Applications, Reviews of Geophysics, 50, Artn Rg4002
10.1029/2012rg000393, 2012.

Liu, X. M., Shaw, J., Liu, T. S., Heller, F., and Yuan, B. Y.: Magnetic Mineralogy of Chinese Loess and Its Significance, Geophys J Int, 108, 301-308, DOI 10.1111/j.1365-246X.1992.tb00859.x, 1992.

Liu, X. M., Rolph, T., Bloemendal, J., Shaw, J., and Liu, T. S.: Remanence characteristics of different magnetic grain size categories at Xifeng, central Chinese Loess Plateau, Quaternary Research, 42, 162-165, 1994.

Liu, X. M., Hesse, P., Rolph, T., and Begét, J. E.: Properties of magnetic mineralogy of Alaskan loess: evidence for pedogenesis, Quatern Int, 62, 93-102, 1999.

Lu, H. Y., and An, Z. S.: Pretreatment methods in loess–palaeosol granulometry, Chinese Science Bulletin, 42, 237-240, 1997.

Machalett, B., Frechen, M., Hambach, U., Oches, E. A., Zoller, L., and Markovic, S. B.: The loess sequence from Remisowka (northern boundary of the Tien Shan Mountains, Kazakhstan) - Part I: Luminescence dating, Quatern Int, 152, 192-201, 10.1016/j.quaint.2005.12.014, 2006.

Machalett, B., Oches, E. A., Frechen, M., Zoller, L., Hambach, U., Mavlyanova, N. G., Markovic, S. B., and Endlicher, W.: Aeolian dust dynamics in central Asia during the Pleistocene: Driven by the long-term migration, seasonality, and permanency of the Asiatic polar front, Geochem Geophy Geosy, 9, Artn Q08q09
10.1029/2007gc001938, 2008.

Maher, B., and Thompson, R.: Paleoclimatic significance of the mineral magnetic record of the Chinese loess and paleosols, Quaternary Research, 37, 155–170, 1992.

Maher, B. A., and Taylor, R. M.: Formation of Ultrafine-Grained Magnetite in Soils, Nature, 336, 368-370, DOI 10.1038/336368a0, 1988.

Maher, B. A., and Thompson, R.: Paleorainfall reconstructions from pedogenic magnetic susceptibility variations in the Chinese loess and paleosols, Quaternary Research, 44, 383-391, DOI 10.1006/qres.1995.1083, 1995.

Maher, B. A.: Magnetic properties of modern soils and Quaternary loessic paleosols: paleoclimatic implications, Palaeogeogr Palaeocl, 137, 25-54, Doi 10.1016/S0031-0182(97)00103-X, 1998.

Maher, B. A.: Palaeoclimatic records of the loess/palaeosol sequences of the Chinese Loess Plateau, Quaternary Sci Rev, 154, 23-84, 2016.

Marković, S. B., Hambach, U., Stevens, T., Jovanović, M., O'Hara-Dhand, K., Basarin, B., Lu, H. Y., Smalley, I., Buggle, B., Zech, M., Svirčev, Z., Sümegi, P., Milojković, N., and Zöller, L.: Loess in the Vojvodina region (Northern Serbia): an essential link between European and Asian Pleistocene environments, Netherlands Journal of Geosciences, 91, 173-188, 2012.

Marković, S. B., Stevens, T., Kukla, G. J., Hambach, U., Fitzsimmons, K. E., Gibbard, P., Buggle, B., Zech, M., Guo, Z., Hao, Q., Wu, H., Dhand, K. O. H., Smalley, I. J., Újvári, G., Sümegi, P., Timar-Gabor, A., Veres, D., Sirocko, F., Vasiljević, D. A., Jary, Z., Svensson, A., Jović, V., Lehmkuhl, F., Kovács, J., and Svirčev, Z.: Danube loess stratigraphy — Towards a pan-European loess stratigraphic model, Earth-Science Reviews, 148, 228–258, 2015.

Mason, J. A., Jacobs, P. M., Greene, R. S. B., and Nettleton, W. D.: Sedimentary aggregates in the Peoria Loess of Nebraska, USA, Catena, 53, 377-397, 10.1016/S0341-8162(03)00073-0, 2003.

Meng, X. M., Derbyshire, E., and Kemp, R. A.: Origin of the magnetic susceptibility signal in Chinese loess, Quaternary Sci Rev, 16, 833-839, Doi 10.1016/S0277-3791(97)00053-X, 1997.

Muhs, D. R., and Bettis, E. A.: Quaternary loess-paleosol sequences as examples of climate-driven sedimentary extremes, Special Papers-Geological Society of America, 53-74, 2003.

Muhs, D. R.: The geologic records of dust in the Quaternary, Aeolian Research, 9, 3-48, 2013.

Nawrocki, J., Wojcik, A., and Bogucki, A.: The magnetic susceptibility record in the Polish and western Ukrainian loess-palaeosol sequences conditioned by palaeoclimate, Boreas, 25, 161-169, 1996.

Nie, J., Song, Y., and King, J. W.: A review of recent advances in red-clay environmental magnetism and paleoclimate history on the Chinese Loess Plateau, Frontiers in Earth Science, 4, 27, 2016.

Nottebaum, V., Lehmkuhl, F., Stauch, G., Hartmann, K., Wunnemann, B., Schimpf, S., and Lu, H. Y.: Regional grain size variations in aeolian sediments along the transition between Tibetan highlands and north-western Chinese deserts - the influence of geomorphological settings on aeolian transport pathways, Earth Surf Proc Land, 39, 1960-1978, 10.1002/esp.3590, 2014.

Nottebaum, V., Stauch, G., Hartmann, K., Zhang, J. R., and Lehmkuhl, F.: Unmixed loess grain size populations along the northern Qilian Shan (China): Relationships between geomorphologic, sedimentologic and climatic controls, Quatern Int, 372, 151-166, 10.1016/j.quaint.2014.12.071, 2015.

Owen, L. A., and Dortch, J. M.: Nature and timing of Quaternary glaciation in the Himalayan-Tibetan orogen, Quaternary Sci Rev, 88, 14-54, 10.1016/j.quascirev.2013.11.016, 2014.

Porter, S. C., and An, Z. S.: Correlation between climate events in the North-Atlantic and China during Last Glaciation, Nature, 375, 305-308, Doi 10.1038/375305a0, 1995.

Prins, M. A.: Glacial and interglacial eolian dust dispersal patterns across the Chinese Loess Plateau inferred from decomposed loess grain-size records, Geochem Geophy Geosy, 8, Artn Q07q05 10.1029/2006gc001563, 2007.

Prins, M. A., Vriend, M., Nugteren, G., Vandenberghe, J., Lu, H. Y., Zheng, H. B., and Weltje, G. J.: Late Quaternary aeolian dust input variability on the Chinese Loess Plateau: inferences from unmixing of loess grain-size records, Quaternary Sci Rev, 26, 230-242, 10.1016/j.quascirev.2006.07.002, 2007.

Prins, M. A., Zheng, H. B., Beets, K., Troelstra, S., Bacon, P., Kamerling, I., Wester, W., Konert, M., Huang, X. T., Ke, W., and Vandenberghe, J.: Dust supply from river floodplains: the case of the lower Huang He (Yellow River) recorded in a loess-palaeosol sequence from the Mangshan Plateau, J Quaternary Sci, 24, 75-84, 10.1002/jqs.1167, 2009.

Pye, K.: Aeolian Dust and Dust Deposits, in, Academic Press, London, 29-62, 1987.

Pye, K., and Zhou, L. P.: Late Pleistocene and Holocene Aeolian Dust Deposition in North China and the Northwest Pacific-Ocean, Palaeogeogr Palaeocl, 73, 11-23, Doi 10.1016/0031-0182(89)90041-2, 1989.

Pye, K.: The nature, origin and accumulation of loess, Quaternary Sci Rev, 14, 653-667, Doi 10.1016/0277-3791(95)00047-X, 1995.

Qiang, M., Lang, L., and Wang, Z.: Do fine-grained components of loess indicate westerlies: Insights from observations of dust storm deposits at Lenghu (Qaidam Basin, China), J Arid Environ, 74, 1232-1239, 10.1016/j.jaridenv.2010.06.002, 2010.

Qin, X. G., Cai, B. G., and Liu, T. S.: Loess record of the aerodynamic environment in the east Asia monsoon area since 60,000 years before present, J Geophys Res-Sol Ea, 110, Artn B01204 10.1029/2004jb003131, 2005.

Rasmussen, S. O., Bigler, M., Blockley, S. P., Blunier, T., Buchardt, S. L., Clausen, H. B., Cvijanovic, I., Dahl-Jensen, D., Johnsen, S. J., Fischer, H., Gkinis, V., Guillevic, M., Hoek, W. Z., Lowe, J. J., Pedro, J. B., Popp, T., Seierstad, I. K., Steffensen, J. P., Svensson, A. M., Vallelonga, P., Vinther, B. M., Walker, M. J. C., Wheatley, J. J., and Winstrup, M.: A stratigraphic framework for abrupt climatic changes during the Last Glacial period based on three synchronized Greenland ice-core records: refining and extending the INTIMATE event stratigraphy, Quaternary Sci Rev, 106, 14-28, 10.1016/j.quascirev.2014.09.007, 2014.

Rea, D. K., Leinen, M., and Janecek, T. R.: Geologic Approach to the Long-Term History of Atmospheric Circulation, Science, 227, 721-725, DOI 10.1126/science.227.4688.721, 1985.

Rea, D. K., and Hovan, S. A.: Grain-Size Distribution and Depositional Processes of the Mineral Component of Abyssal Sediments - Lessons from the North Pacific, Paleoceanography, 10, 251-258, Doi 10.1029/94pa03355, 1995.

Rousseau, D. D., Sima, A., Antoine, P., Hatté, C., Lang, A., and Zöller, L.: Link between European and North Atlantic abrupt climate changes over the last glaciation, Geophys Res Lett, 34, 22, 2007.

Smalley, I.: Making the material: The formation of silt-sized primary mineral particles for loess deposits, Quaternary Sci Rev, 14, 645-651, Doi 10.1016/0277-3791(95)00046-1, 1995.

Smalley, I. J., Mavlyanova, N. G., Rakhmatullaev, K. L., Shermatov, M. S., Machalett, B., Dhand, K. O., and Jefferson, I. F.: The formation of loess deposits in the Tashkent region and parts of Central Asia; and problems with irrigation, hydrocollapse and soil erosion, Quatern Int, 152, 59-69, 10.1016/j.quaint.2005.12.002, 2006.

Song, Y. G., Shi, Z. T., Fang, X. M., Nie, J. S., Naoto, I., Qiang, X. K., and Wang, X. L.: Loess magnetic properties in the Ili Basin and their correlation with the Chinese Loess Plateau, Sci China Earth Sci, 53, 419-431, 10.1007/s11430-010-0011-5, 2010.

Song, Y. G., Li, C. X., Zhao, J. D., Cheng, P., and Zeng, M. X.: A combined luminescence and radiocarbon dating study of the Ili loess, Central Asia, Quat Geochronol, 10, 2-7, 10.1016/j.quageo.2012.04.005, 2012.

Song, Y. G., Chen, X. L., Qian, L. B., Li, C. X., Li, Y., Li, X. X., Chang, H., and An, Z. S.: Distribution and composition of loess sediments in the Ili Basin, Central Asia, Quatern Int, 334, 61-73, 10.1016/j.quaint.2013.12.053, 2014.

Song, Y. G., Lai, Z. P., Li, Y., Chen, T., and Wang, Y. X.: Comparison between luminescence and radiocarbon dating of late Quaternary loess from the Ili Basin in Central Asia, Quat Geochronol, 30, 405-410, 10.1016/j.quageo.2015.01.012, 2015.

Stevens, T., Adamiec, G., Bird, A. F., and Lu, H. Y.: An abrupt shift in dust source on the Chinese Loess Plateau revealed through high sampling resolution OSL dating, Quaternary Sci Rev, 82, 121-132, 10.1016/j.quascirev.2013.10.014, 2013.

Stevens, T., Buylaert, J. P., Lu, H., Thiel, C., Murray, A., Frechen, M., Yi, S., and Zeng, L.: Mass accumulation rate and monsoon records from Xifeng, Chinese Loess Plateau, based on a luminescence age model, J Quaternary Sci, 31, 391-405, 2016.

Sun, D.: Monsoon and westerly circulation changes recorded in the late Cenozoic aeolian sequences of Northern China, Global Planet Change, 41, 63-80, 10.1016/j.gloplacha.2003.11.001, 2004.

Sun, D. H., Bloemendal, J., Rea, D. K., Vandenberghe, J., Jiang, F. C., An, Z. S., and Su, R. X.: Grain-size distribution function of polymodal sediments in hydraulic and aeolian environments, and numerical partitioning of the sedimentary components, Sediment Geol, 152, 263-277, Pii S0037-0738(02)00082-9
Doi 10.1016/S0037-0738(02)00082-9, 2002.

Sun, D. H., Chen, F. H., Bloemendal, J., and Su, R. X.: Seasonal variability of modern dust over the Loess Plateau of China, J Geophys Res-Atmos, 108, Artn 4665
10.1029/2003jd003382, 2003.

Sun, D. H., Bloemendal, J., Rea, D. K., An, Z. S., Vandenberghe, J., Lu, H. Y., Su, R. X., and Liu, T. S.: Bimodal grain-size distribution of Chinese loess, and its palaeoclimatic implications, Catena, 55, 325-340, 10.1016/S0341-8162(03)00109-7, 2004.

Sun, D. H.: Supper-fine grain size components in Chinese loess and their palaeoclimatic implication, Quaternary Sciences, 26, 928-936 (in Chinese with English abstract), 2006.

Sun, Y., Lu, H., and An, Z.: Grain size distribution of quartz isolated from Chinese loess1 paleosol, Chinese Science Bulletin, 45, 2296-2298, 2000a.

Sun, Y., Clemens, S. C., An, Z., and Yu, Z.: Astronomical timescale and palaeoclimatic implication of stacked 3.6-Myr monsoon records from the Chinese Loess Plateau, Quaternary Sci Rev, 25, 33-48, 2006a.

Sun, Y., Lu, H. Y., and An, Z. S.: Grain size of loess, palaeosol and Red Clay deposits on the Chinese Loess Plateau: Significance for understanding pedogenic alteration and palaeomonsoon evolution, Palaeogeogr Palaeocl, 241, 129-138, 10.1016/j.palaeo.2006.06.018, 2006b.

Sun, Y., Clemens, S. C., Morrill, C., Lin, X., Wang, X., and An, Z.: Influence of Atlantic meridional overturning circulation on the East Asian winter monsoon, Nature Geoscience, 5, 46-49, 2012.

Sun, Y. B., Lu, H. Y., and An, Z. S.: Grain size distribution of quartz isolated from Chinese loess/paleosol, Chinese Science Bulletin, 45, 2296-2298, Doi 10.1007/Bf02886372, 2000b.

Sun, Y. B., Wang, X. L., Liu, Q. S., and Clemens, S. C.: Impacts of post-depositional processes on rapid monsoon signals recorded by the last glacial loess deposits of northern China, Earth and Planetary Science Letters, 289, 171-179, 10.1016/j.epsl.2009.10.038, 2010.

Tsoar, H., and Pye, K.: Dust Transport and the Question of Desert Loess Formation, Sedimentology, 34, 139-153, DOI 10.1111/j.1365-3091.1987.tb00566.x, 1987.

Ujvari, G., Kok, J. F., Varga, G., and Kovacs, J.: The physics of wind-blown loess: Implications for grain size proxy interpretations in Quaternary paleoclimate studies, Earth-Science Reviews, 154, 247-278, 10.1016/j.earscirev.2016.01.006, 2016.

Vandenberghe, J., Renssen, H., van Huissteden, K., Nugteren, G., Konert, M., Lu, H. Y., Dodonov, A., and Buylaert, J. P.: Penetration of Atlantic westerly winds into Central and East Asia, Quaternary Sci Rev, 25, 2380-2389, 10.1016/j.quascirev.2006.02.017, 2006.

Vandenberghe, J.: Grain size of fine-grained windblown sediment: A powerful proxy for process identification, Earth-Science Reviews, 121, 18-30, 10.1016/j.earscirev.2013.03.001, 2013.

Varga, G.: Similarities among the Plio-Pleistocene terrestrial aeolian dust deposits in the World and in Hungary, Quatern Int, 234, 98-108, 10.1016/j.quaint.2010.09.011, 2011.

Vriend, M., and Prins, M. A.: Calibration of modelled mixing patterns in loess grain-size distributions: an example from the north-eastern margin of the Tibetan Plateau, China, Sedimentology, 52, 1361-1374, 10.1111/j.1365-3091.2005.00743.x, 2005.

Vriend, M.: Lost in loess: Late Quaternary eolian dust dispersal patterns across Central China inferred from decomposed loess grain-size records, Amsterdam, VU University, The Netherlands, 53 pp., 2007.

Vriend, M., Prins, M. A., Buylaert, J. P., Vandenberghe, J., and Lu, H. Y.: Contrasting dust supply patterns across the north-western Chinese Loess Plateau during the last glacial-interglacial cycle, Quatern Int, 240, 167-180, 10.1016/j.quaint.2010.11.009, 2011.

Wang, H., Mason, J. A., and Balsam, W. L.: The importance of both geological and pedological processes in control of grain size and sedimentation rates in Peoria Loess, Geoderma, 136, 388-400, 10.1016/j.geoderma.2006.04.005, 2006.

Xiao, J., Porter, S. C., An, Z. S., Kumai, H., and Yoshikawa, S.: Grain-Size of Quartz as an Indicator of Winter Monsoon Strength on the Loess Plateau of Central China during the Last 130,000-Yr, Quaternary Research, 43, 22-29, DOI 10.1006/qres.1995.1003, 1995.

Yang, S. L., Ding, F., and Ding, Z. L.: Pleistocene chemical weathering history of Asian arid and semi-arid regions recorded in loess deposits of China and Tajikistan, Geochim Cosmochim Ac, 70, 1695-1709, 10.1016/j.gca.2005.12.012, 2006.

Yang, S. L., and Ding, Z. L.: A 249 kyr stack of eight loess grain size records from northern China documenting millennial-scale climate variability, Geochem Geophy Geosy, 15, 798-814, 10.1002/2013gc005113, 2014.

Ye, W.: Characteristics of physical environment and conditions of loess formation in Yili area, Xinjiang, Arid Land Geography, 22, 9-16 (in Chinese), 1999.

Ye, W., Sang, C., and Zhao, X.: Spatial-temporal distribution of loess and source of dust in Xinjiang, Journal of Desert Research, 23, 514-520 (in Chinese), 2003.

Youn, J. H., Seong, Y. B., Choi, J. H., Abdrakhmatov, K., and Ormukov, C.: Loess deposits in the northern Kyrgyz Tien Shan: Implications for the paleoclimate reconstruction during the Late Quaternary, Catena, 117, 81-93, 10.1016/j.catena.2013.09.007, 2014.

Yu, S. Y., Colman, S. M., and Li, L. X.: BEMMA: A Hierarchical Bayesian End-Member Modeling Analysis of Sediment Grain-Size Distributions, Math Geosci, 48, 723-741, 10.1007/s11004-015-9611-0, 2016.

Zech, R.: A late Pleistocene glacial chronology from the Kitschi-Kurumdu Valley, Tien Shan (Kyrgyzstan), based on Be-10 surface exposure dating, Quaternary Research, 77, 281-288, 10.1016/j.yqres.2011.11.008, 2012.

Zeeden, C., Hambach, U., Veres, D., Fitzsimmons, K., Obreht, I., Bösken, J., and Lehmkuhl, F.: Millennial scale climate oscillations recorded in the Lower Danube loess over the last glacial period, Palaeogeography, Palaeoclimatology, Palaeoecology, (in press), 2016.

Zhang, X. J., Jin, L. Y., Huang, W., and Chen, F. H.: Forcing mechanisms of orbital-scale changes in winter rainfall over northwestern China during the Holocene, Holocene, 26, 549-555, 10.1177/0959683615612569, 2016.

Zhang, X. Y., Arimoto, R., and An, Z. S.: Glacial and interglacial patterns for Asian dust transport, Quaternary Sci Rev, 18, 811-819, Doi 10.1016/S0277-3791(98)00028-6, 1999.

Zhou, L. P., Oldfield, F., Wintle, A. G., Robinson, S. G., and Wang, J. T.: Partly Pedogenic Origin of Magnetic Variations in Chinese Loess, Nature, 346, 737-739, DOI 10.1038/346737a0, 1990.

Clim. Past Discuss., doi:10.5194/cp-2017-50, 2017
Manuscript under review for journal Clim. Past
Discussion started: 27 March 2017


Climate of the Past
Discussions
Open Access
EGU

Fig01

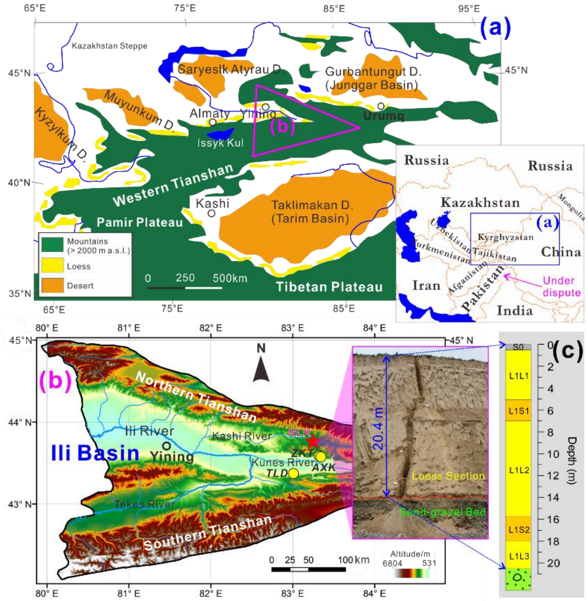

Clim. Past Discuss., doi:10.5194/cp-2017-50, 2017
Manuscript under review for journal Clim. Past
Discussion started: 27 March 2017


Climate of the Past Discussions

Fig02

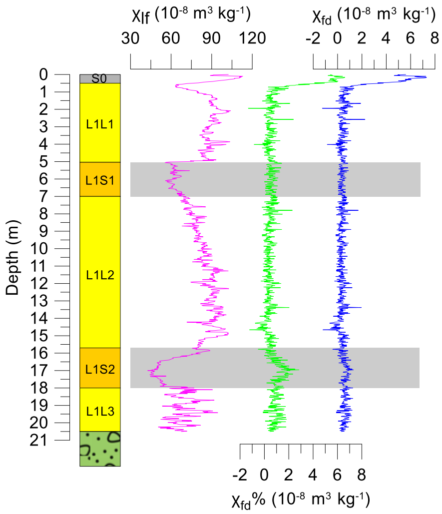

Clim. Past Discuss., doi:10.5194/cp-2017-50, 2017
Manuscript under review for journal Clim. Past
Discussion started: 27 March 2017


Climate of the Past Discussions
Open Access

Fig03

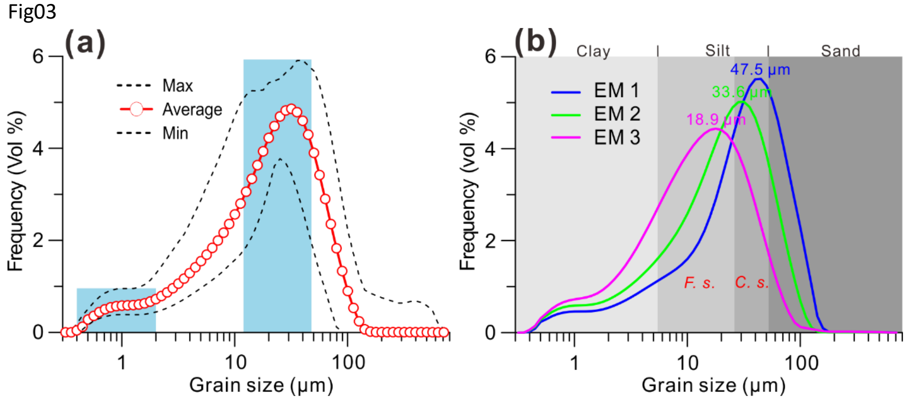

Clim. Past Discuss., doi:10.5194/cp-2017-50, 2017
Manuscript under review for journal Clim. Past
Discussion started: 27 March 2017


Fig04

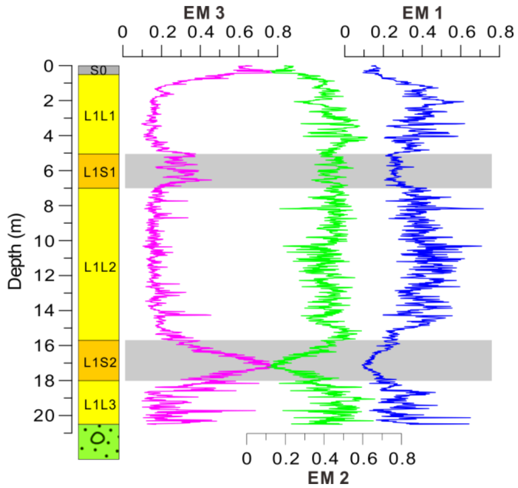

Clim. Past Discuss., doi:10.5194/cp-2017-50, 2017
Manuscript under review for journal Clim. Past
Discussion started: 27 March 2017


Climate of the Past Discussions
Open Access

Fig05

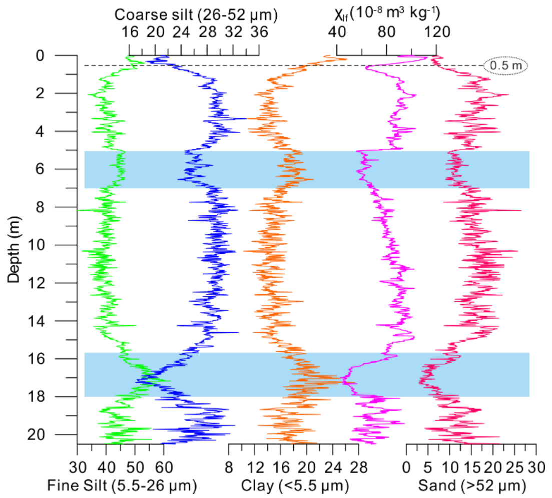

Clim. Past Discuss., doi:10.5194/cp-2017-50, 2017
Manuscript under review for journal Clim. Past
Discussion started: 27 March 2017


Climate of the Past Discussions

Fig06

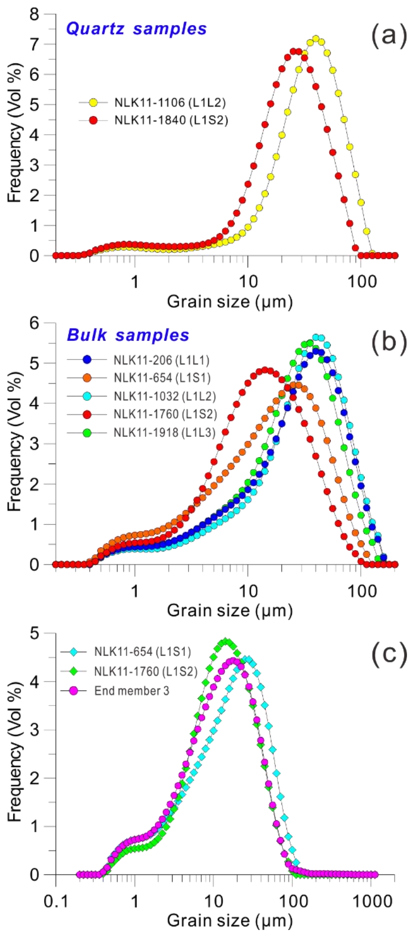

Fig07

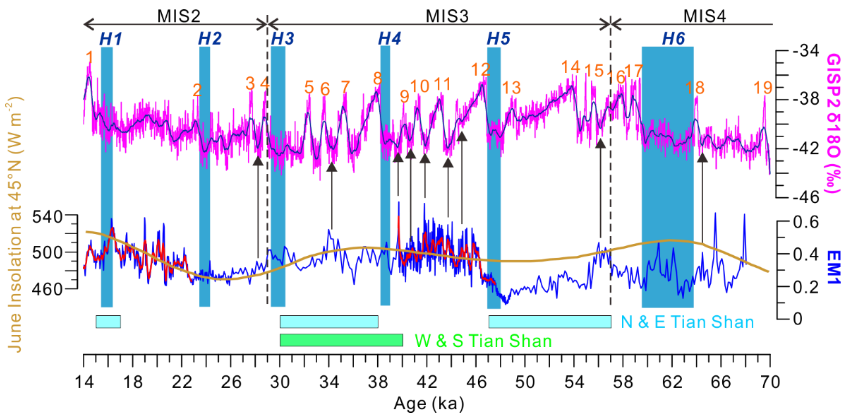
MIS2
MIS3
MIS4
H1
H2
H3
H4
H5
H6
GISP2 δ18O (‰)
EM1
June Insolation at 45°N (W m⁻²)
N & E Tian Shan
W & S Tian Shan
Age (ka)